Revista de Chimie
https://revistadechimie.ro
https://doi.org/10.37358/Rev.Chim.1949

Preparation and Characterization of Polyethyleneimine/ Moliybdenum Disufide Composite for Hexavalent Chromium Removal from Aqueous Systems

WEI WEI LIN[1], MIAO SHAN TANG[1], JIAN HUA CHEN[1,2*], YANG HUANG[1], QIAO JING LIN[1], YONG DONG HUANG[3]

[1]College of Chemistry, Chemical Engineering and Environment, Minnan Normal University, Zhangzhou 363000, China
[2]Fujian Province University Key Laboratory of Modern Analytical Science and Separation Technology, Minnan Normal University, Zhangzhou 363000, China
[3]National Key Laboratory of Biochemical Engineering, Institute of Process Engineering, Chinese Academy of Sciences, Beijing, 100190, PR China.

Abstract**:** *In this experiment, polyethyleneimine (PEI) was used to modify the surface of flower-like molybdenum disulfide, and the PEI/MoS_2 adsorbent was successfully synthesized and applied to remove Cr(VI) from wastewater. The physical and chemical property of PEI/MoS_2 were analyzed by TEM, SEM and FTIR, etc. The affecting factors of the adsorption of Cr(VI) by PEI/MoS_2 were discussed, including the effects of PEI loading, concentration of Cr(VI), pH value, etc. When the solution temperature is 25 ^oC, the solution pH is 2, the concentration of* PEI/MoS_2 composites adsorbent and *Cr(VI)* solution *are 0.1 g/L and 50 mg/L, respectively, the adsorption amount of Cr(VI) by PEI/MoS_2-10 is 120.7 mg/g. Experiments show that PEI/MoS_2-10 has a strong selectivity to Cr(VI), and regeneration experiments show that PEI/MoS_2 has a high reusable.*

Keywords**:** *flower molybdenum disulfide, polyethyleneimine, hexavalent chromium, adsorption*

1. Introduction

With the acceleration of the modernization process and the development of industrialization, overusing of heavy metals has led to grim pollution [1,2]. Chromium is commonly used in industrial production, and it has produced a large amount of chromium-containing sewage mainly containing hexavalent chromium Cr(VI). Cr(VI) is high toxicity, carcinogenicity, mutagenic ability, non-biodegradability and long-lasting harm to the environment [3]. On the contrary, trivalent chromium (Cr(III)) is much less toxicity and is one of the essential trace element for humans [4,5]. Thus, it is necessary to recover and reduce Cr(VI) to Cr(III). Scholars have also conducted more and more researches on chromium-containing wastewater treatment methods. There are many removal methods, such as electrochemical [6], chemical precipitation [7], membrane separation [8], ion exchange [9], biological method [10] and adsorption [11-13]. Adsorption is the main method to remove Cr(VI) pollutants in water. Numerous adsorbents, including fly ash [14], activated carbon [15,16], chitosan [17], attapulgite rod [18], zeolite [19], and polymer [20] have been used. However, most adsorbents still have obvious disadvantages, such as high cost or inefficient adsorption performance. Therefore, developing low-cost and high-efficiency adsorbents is required.

Molybdenum disulfide (MoS2) is the main component of molybdenite, and is a layered mineral, belonging to the hexagonal or rhombic system [21]. Due to this unique structure and properties, it can be widely used in various fields, such as lubricant [22,23], electrode materials [24]. MoS2 has high reactivity, it can be used as a catalyst material [25]. In addition, MoS2 has much exposed S atoms on the surface, while sulfur has a strong adhesion to metals, which is expected to adsorption heavy metal in the water environment [26-28]. However, there are insufficient adsorption sites for molybdenum disulfide

**email:jhchen73@126.com*

as an adsorbent. It is usually used to introduce other functional groups [29,30] or to compound with other materials to improve the adsorption capacity of MoS2 [31,32].

Polyethyleneimine (PEI) is a typical polyamine [33]. It has high reactivity and has many functional groups that can be combined with metal ions. In order to make PEI more suitable for environmental pollution treatment, it can be loaded on other materials to form composite materials to overcome the shortcomings of being easily soluble in water and difficult to recycle [34-36].

Because PEI is very soluble in water, it can not be reused when it is used to remove metal ions from wastewater. Pure MoS_2 nanomaterials have the defects of insufficient functional sites. Therefore, in this study, using flower molybdenum disulfide as a carrier, PEI/MoS_2 composite adsorbent was prepared by immobilized PEI onto the surface of MoS_2. The important influence factors, include reaction time, original Cr(VI) concentration, *p*H value and temperature of solution on PEI/MoS_2 adsorption properties were discussed. The adsorption mechanism and reusability of PEI/MoS_2 was also investigated.

2. Materials and methods

2.1. Materials

Diphenyl carbamide was purchased at Sinopharm Chemical Reagent Co., Ltd. The polyethyleneimine (MW = 1800) was purchased from Macklin. All other chemicals were from Xilong Chemical Co., Ltd.

2.2. Preparation of PEI/MoS_2 composites adsorbent

1.44 g of sodium molybdate dihydrate ($Na_2MoO_4 \cdot 2H_2O$) and 1.8268 g of thiourea (NH_2CSNH_2) were put into a beaker, and then add certain amount of deionized water to dissolve. Then add hydrochloric acid to adjust the acidity to *p*H = 1.5. The obtained solution was placed in a 100 mL reactor and then reacted in a 230°C oven for 20 h. The product was collected by centrifuged at 10,000 rpm. finally, flower molybdenum disulfide MoS_2 was prepared.

Prepare 100 mL PEI solutions with a concentration of 5, 10, 15, 20 and 25 mg/mL. MoS_2 was immersed in an ultrasonic bath for 10 min in the above PEI solutions, stirred at 25°C for 12 h, separated by suction filtration. MoS_2 with different PEI loading ratios is recorded as PEI/MoS_2-X (X = 5, 10, 15, 20, 25).

2.3. Characterization

The morphology of MoS_2 and PEI/MoS_2 composites adsorbent was observed using a scanning electron microscope (SEM, Hitachi S-3400N) and transmission electron microscope (TEM, JEM-2100). The physico-chemical property of MoS_2 and PEI/MoS_2-10 was analyzed by Fourier-transformed infrared spectroscopy (FTIR, Necolet360) and X-ray Diffraction (XRD, D8 Advance). X-ray photoelectron spectroscopy (XPS, K-Alpha+) was used to determine the surface composition of the adsorbent. The specific surface area of PEI/MoS_2 was studied by the Brunauer-Emmett-Teller (BET) with an N_2-adsorpmeter.

2.4. Adsorption experiments

The Cr(VI) in the experiment is from potassium dichromate. Appropriate Cr(VI) solutions were added to 50 mL polyethylene vials, and kept PEI/MoS_2 composites of 0.1 g/L and shaken for enough time at 25°C in the shaker. Finally, the solutions were centrifuged separation. We measured Cr(VI) concentrations of supernate through the 1,5-diphenylcarbohydrazide spectrophotometric method with UV-vis spectrophotometer (λmax = 540 nm). The adsorption amounts of PEI/MoS_2 composites adsorbent were calculated as:

$$q_e = (C_0 - C_e)V / m \quad (1)$$

where C_0 and C_e (mg/L) are the original concentrations and equilibrium concentrations of Cr(VI) solution, respectively; V (mL) is the volume of Cr(VI) solutions; and m (mg) is the dry weight of PEI/MoS_2 composites.

All data in this experiment were measured three times and averaged.

3. Results and discussions

3.1. Characterization

3.1.1. SEM and TEM study

Figure 1a shows that the size of the flower MoS_2 is about 200 nm. It is composed of many ultrathin nanosheets. From Figure 1a we also can see that the surface of flower MoS_2 is smooth and has a certain degree of curling, which makes it have more adsorption sites. After loading PEI, as shown in Figure 1b, the PEI/MoS_2-10 surface became rough. Compare Figure 1c and d, PEI/MoS_2-10 nanosheets become thicker than MoS_2 after loading PEI.

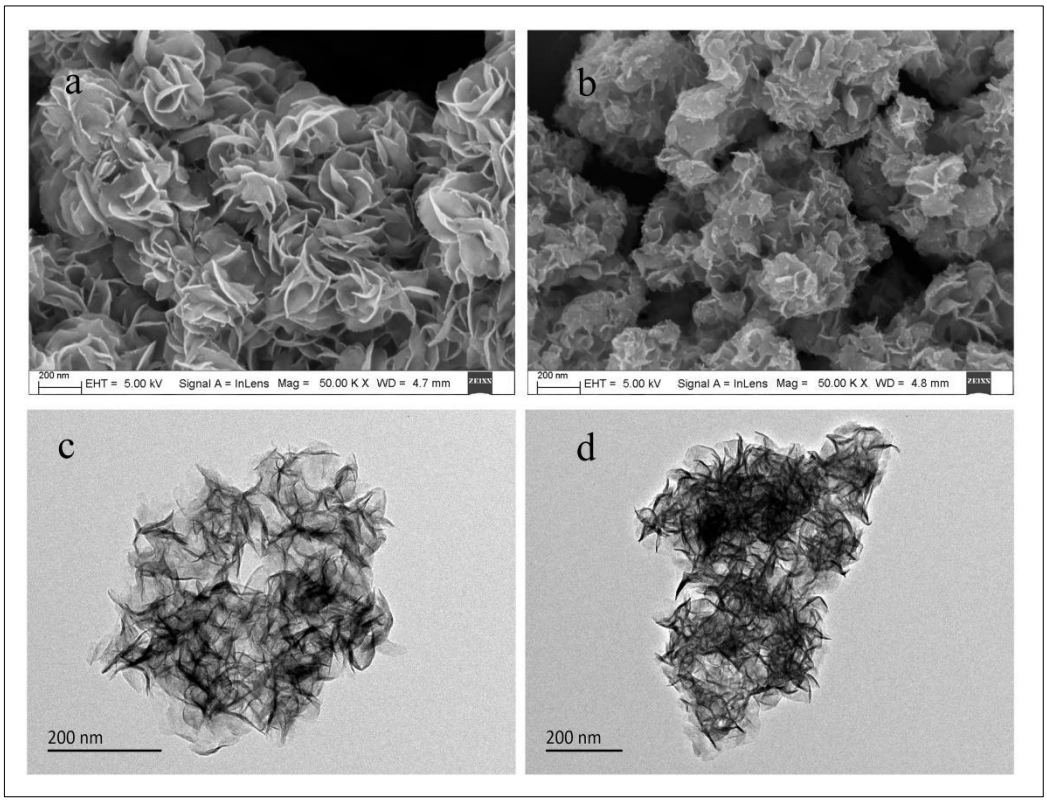

Figure 1. SEM images of: (a)MoS_2, (b)PEI/MoS_2-10;
TEM images of: (c)MoS_2, (d)PEI/MoS_2-10

3.1.2. XRD analysis

XRD images of MoS_2 and PEI/MoS_2-10 are exposed in Figure 2. It showed that the diffraction peaks of the sample are 13.9°, 32.7°, 39.4° and 58.7°, which correspond to the positions of the characteristic diffraction peaks (002), (100), (103) and (110) in the molybdenum disulfide standard card (PDF#75-1539), respectively. This indicates that MoS_2 was successfully synthesized and highly crystallized. The XRD diffraction peak position and peak intensity of PEI/MoS_2-10 and MoS_2 are consistent, implying that the loading of PEI will not affect the structure of MoS_2.

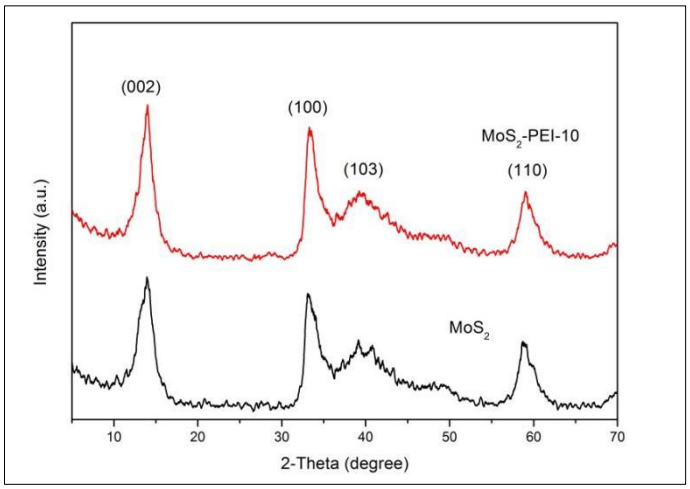

Figure 2. XRD patterns of MoS_2 and PEI/MoS_2-10 composites

3.1.3. FTIR characterization

The resulting FTIR spectra for MoS_2 and PEI/MoS_2-10 are displayed in Figure 3. The corresponding Mo-S peak centered at 560 cm^{-1}, and the stretching vibration of C-N in the PEI framework can be seen at 1384 cm^{-1} [37]. The absorption peaks of amide groups were observed at 1520 and 1634 cm^{-1} [38], and the characteristic peaks appearing at 2960 cm^{-1} were related to the methylene of PEI, which proved that PEI has been successfully loaded on the MoS_2. O-H stretching vibration can be seen at 3432 cm^{-1}, which may be physically adsorbed water molecules [38].

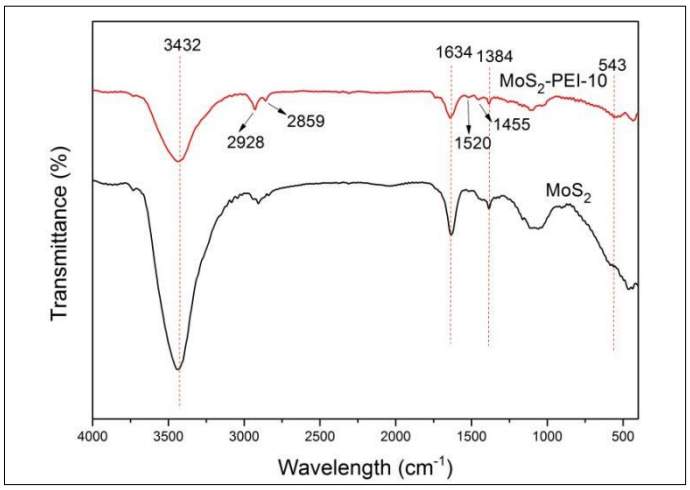

Figure 3. FTIR spectra of MoS_2 and PEI/MoS_2-10

3.1.4. BET characterization

The specific surface area of adsorbent directly affects the contact probability between the adsorbent and Cr(VI), and the larger the specific surface area, the higher the contact probability. The specific surface area of MoS_2, PEI/MoS_2-10, PEI/MoS_2-15, PEI/MoS_2-20 and PEI/MoS_2-25 were analyzed and displayed in Figure 4. The specific surface area of them are 94.663 m^2/g, 122.973 m^2/g, 45.466 m^2/g, 40.234 m^2/g and 39.257 m^2/g, respectively. PEI/MoS_2-10 has the largest specific surface area. This is because the proper loading of PEI increases the specific surface area and provides more adsorption sites. However, excessive loading of PEI on the MoS_2 led to sharp decrease of surface area, which results in the blocking of the lamellar gap of MoS_2 by the PEI.

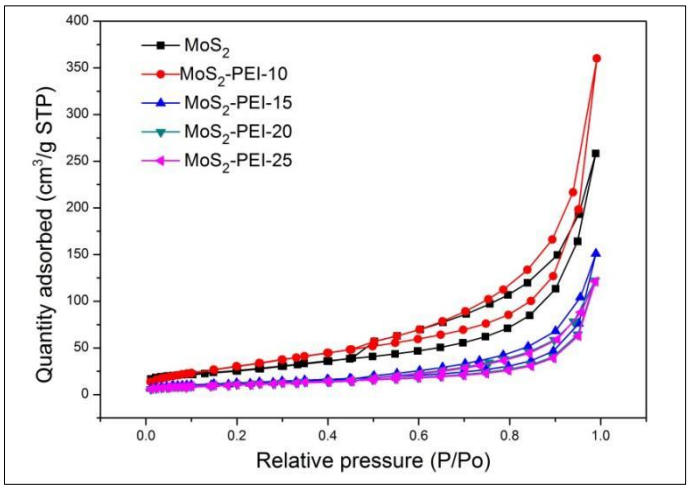

Figure 4. Nitrogen adsorption-desorption isotherms of MoS_2 and MoS_2-PEI-X

3.2. Effect of PEI loading on Cr(VI) adsorption

We selected five different PEI loadings of PEI/MoS_2 for adsorption experiments to research the effect of PEI loading on Cr(VI) adsorption performance of PEI/MoS_2 composites adsorbent. Figure 5 shows that adsorption property of PEI/MoS_2 for Cr(VI) was significantly improved after PEI was loaded on MoS_2. When PEI is loaded on MoS_2, many amino groups (-NH_2) and imino groups (=NH) on PEI are also introduced into PEI/MoS_2, thus enhancing the adsorption property of PEI/MoS_2 for Cr(VI). When further adding of PEI loading from PEI/MoS_2-10 to PEI/MoS_2-25, the adsorption capacity of PEI/MoS_2-X decreased. The excessive loading of PEI blocks the laminar gaps of MoS_2, which reduces the adsorption capacity. Follow-up experiments select PEI/MoS_2-10 for research.

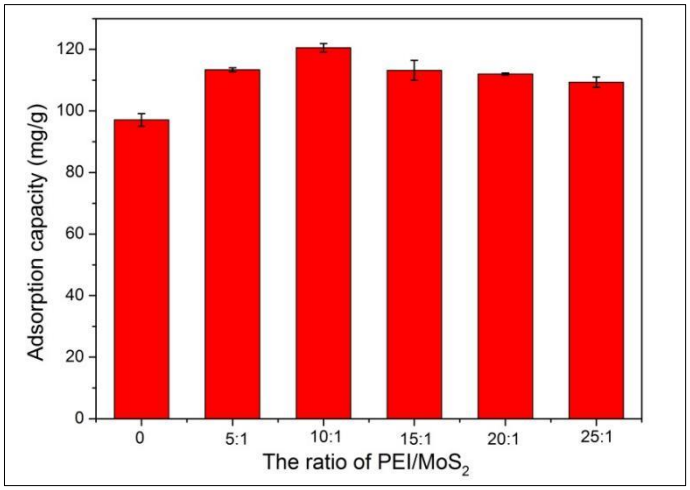

Figure 5. Effect of PEI loading on PEI/MoS_2-X composites adsorbent on Cr(VI) adsorption

3.3. Adsorption kinetics

Figure 6 shows the changing of adsorption capacity PEI/MoS_2-10 in Cr(VI) solutions with an original concentration of 30, 50 and 70 mg/L. It is shown that the adsorption capacity of PEI/MoS_2-10 for Cr(VI) increased sharply within the first hour, and then increased slowly with the adsorption time. This can be credited to the amino group (-NH_2) and imino group (=NH) on the surface of the PEI/MoS_2-10 provided numerous adsorption sites at the beginning of the adsorption, and the concentration of Cr(VI) was also at the original state. At this time, there is a large concentration difference between solvent and the solute, and the adsorption driving force is large. The rise of the adsorption amount becomes slower with time,

due to the concentration difference decreases and the driving force weakens. And then the equilibrium state is basically reached after 6 h of adsorption. Therefore, the subsequent experiments used 6 h as the adsorption time for the adsorption equilibrium.

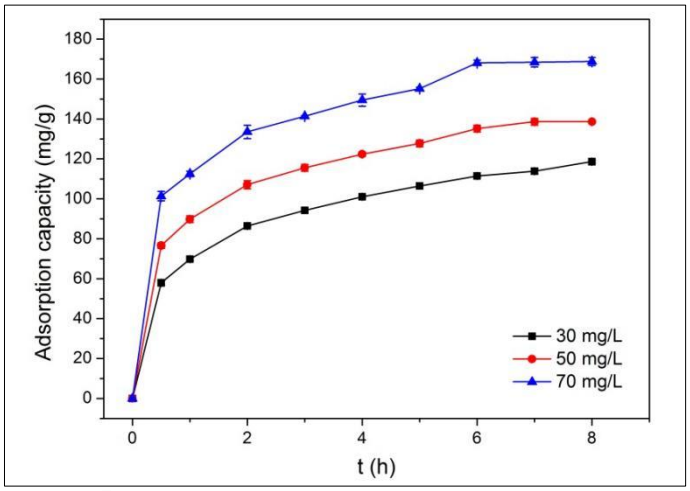

Figure 6. Effect of adsorption time on Cr(VI) adsorption by PEI/MoS_2-10 at temperature of 25°C

We conducted the pseudo-first-order and pseudo-second-order kinetic model to characterize the adsorption behaviors.

Pseudo-first-order dynamic model equation:

$$q_t = q_e(1 - e^{-k_1 t}) \quad (2)$$

Pseudo-second-order dynamic model equations:

$$t/q_t = 1/k_2 q_e^2 + t/q_e \quad (3)$$

where q_e (mg/g) is the adsorption amount at equilibrium; q_t (mg/g) is the adsorption amount at time t; k_1 (min^{-1}) is the rate constant of the pseudo-first-order kinetic model; k_2 (g/mg·min) is the rate constant of the pseudo-second-order kinetic model.

Table 1 shows the fitting results. It indicates that the correlation coefficient of pseudo-second-order kinetics is significantly higher than that of pseudo-first-order kinetics, and the calculated equilibrium adsorption capacity is nearer to the actual test results. From the Figure 7, it can be seen intuitively that the fitting results of the pseudo-second-order kinetics are more consistent with the experimental data, and the calculated equilibrium adsorption capacity is closer to the actual test results. Thus, the process of PEI/MoS_2-10 adsorption of Cr(VI) is more in line with the pseudo-second-order kinetic model, which indicates that the adsorption process is a chemical adsorption.

Table 1. Kinetic parameters of Cr(VI) adsorption by PEI/MoS_2-10

		pseudo-first-order kinetic model			pseudo-second-order kinetic model		
C_o (mg/L)	q_{exp} (mg/g)	q_{cal}	k_1	R^2	q_{cal} (mg/g)	k_2	R^2
30	118.6	108.3	1.05731	0.9482	122.6	0.01338	0.9884
50	138.6	129.0	1.31280	0.9465	144.7	0.01390	0.9919
70	168.8	156.8	1.52268	0.9373	175.6	0.01259	0.9920

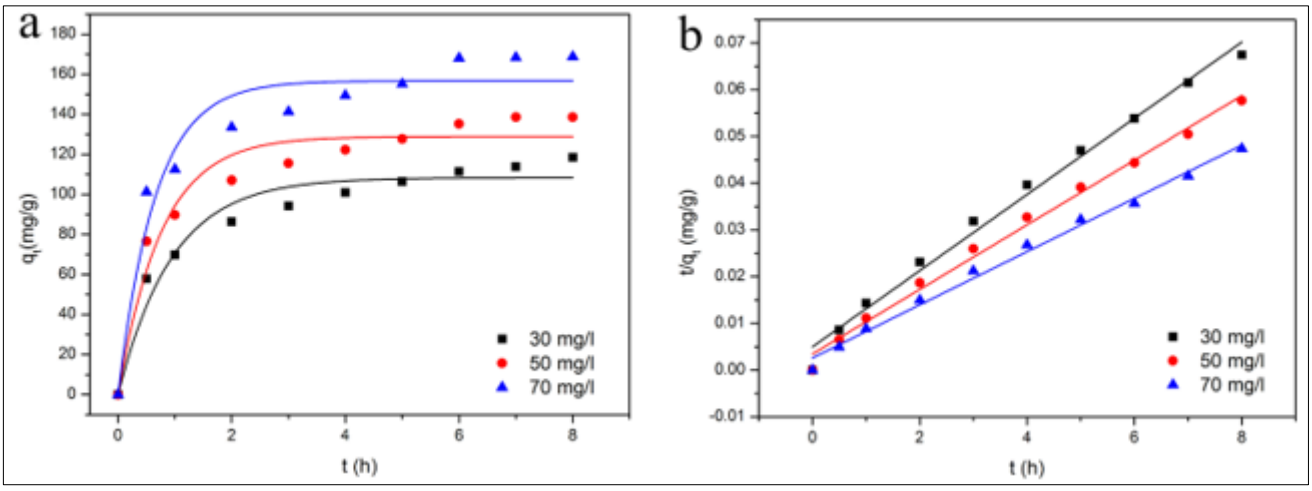

Figure 7. Kinetic model: (a) pseudo-first-order kinetic equation curve; (b) pseudo-second-order kinetic equation curve

3.4. Effect of *p*H on Cr(VI) adsorption

The *p*H of solution affects the existence of metal ions in the aqueous solution as well as the charge density on the surface of the adsorbent. According to the various *p*H of the solution, Cr(VI) in water principally has five forms: $Cr_2O_7^{2-}$, $HCr_2O_7^-$, CrO_4^{2-}, $HCrO_4^-$ and H_2CrO_4. When 2 < *p*H < 6, Cr(VI) principally occurs in the form of $HCrO_4^-$ and $Cr_2O_7^{2-}$; *p*H > 6, it principally occurs in the form of CrO_4^{2-} [38]. The effect of *p*H value on PEI/MoS_2-10 composites adsorbent on Cr(VI) adsorption is shown in Figure 8 When the solution *p*H = 2, the adsorption amount of PEI/MoS_2-10 to Cr(VI) reached the maximum, and the adsorption amount decreased as the *p*H value increased. This is because the amino group (-NH_2) on the surface of PEI/MoS_2-10 will be protonated (-NH_3^+) at a low *p*H value, making the surface of the PEI/MoS_2-10 positively charged, and then the electrostatic force between PEI/MoS_2-10 and negatively charged Cr(VI) is enhanced. As shown in Figure 9, the PZC of PEI/MoS_2-10 is 5.6. With the increase of solution *p*H value (higher than 5.6), the surface group of PEI/MoS_2-10 is deprotonated, resulting in the surface of PEI/MoS_2-10 being negatively charged and causing electrostatic repulsion with the anion form of Cr(VI). In addition, a large amount of OH^- will compete with the negatively charged Cr(VI) for adsorption sites on the surface of PEI/MoS_2-10 [39], which greatly reduces the amount of Cr(VI) adsorption.

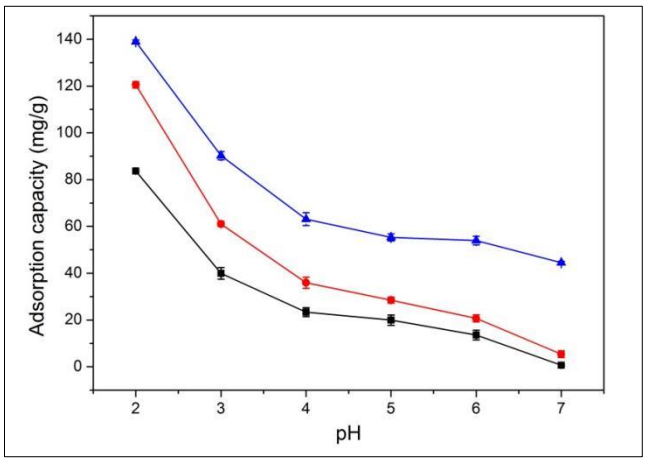

Figure 8. Effect of solution *p*H on Cr(VI) adsorption by PEI/MoS_2-10, temperature of 25°C, adsorption time of 6 h

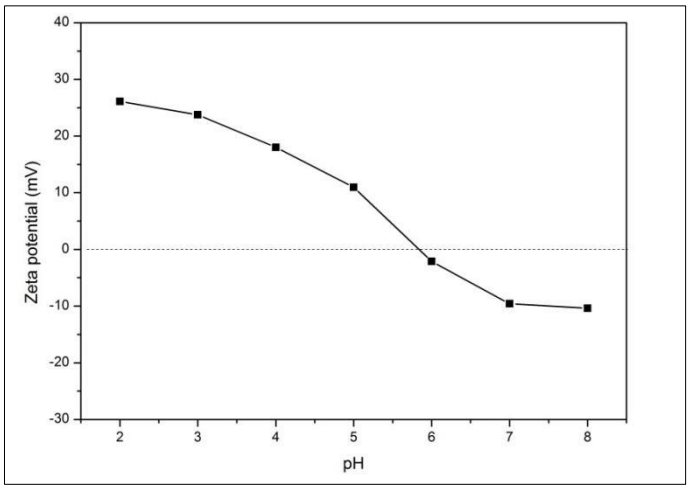

Figure 9. PZC of PEI/MoS_2-10

3.5. Competitive adsorption

Besides Cr(VI), other metal ions also exist in the actual water samples at the same time, so it is very meaningful to study the change of adsorption property of PEI/MoS_2-10 for Cr(VI) in the presence of multiple ions. Here, add coexist ions to analyze the change of adsorption performance of PEI/MoS_2-10 for Cr(VI). Figure 10 shows the influence of coexist ions on the adsorption properties of PEI/MoS_2-10. Due to the influence of coexisting ions, the adsorption capacity of PEI/MoS_2-10 for Cr(VI) decreased slightly, which was due to the co-exist ion competition for adsorption sites. However, compared with the other three metal ions, PEI/MoS_2-10 still shows strong selectivity for Cr(VI). This is because PEI/MoS_2-10 has many amino and imino groups. These groups are protonated at low *p*H value, which makes the surface positively charged and easier to combine with negatively charged Cr(VI) through electrostatic interaction, while Co(II), Zn(II) and Cd(II) in solution coexist in the form of positively charged ions, it can combine with amino group and imino group through complexation reaction, thus occupying the adsorption site. However, it has electrostatic repulsion with protonated PEI/MoS_2-10, so the adsorption capacity is low.

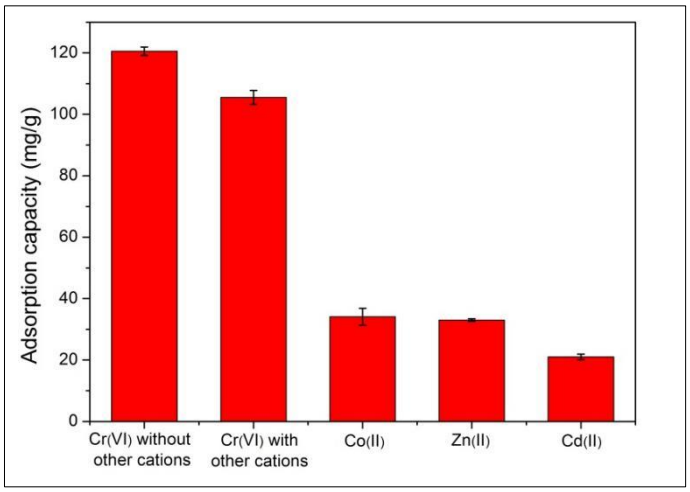

Figure 10. Effect of interference ion on Cr(VI) adsorption by PEI/MoS_2-10, solution *p*H of 2, temperature of 25°C, adsorption time of 6 h

3.6. Adsorption isotherms

Figure 11 illustrates the influence of original concentration of Cr(VI) solution. It shows that the adsorption amount is smaller for lower Cr(VI) concentration. The possible reason is that the binding site on PEI/MoS_2-10 cannot be fully utilized at a lower ion concentration.

Freundlich and Langmuir isotherm models are used to fit the experimental data. The Freundlich isotherm adsorption model describes heterogeneous adsorption, assuming that the multi-layer adsorption. The Langmuir isotherm model assumes monolayer adsorption.

Freundlich isotherm adsorption model:

$$q_e = K_f C_e^{1/n} \quad (4)$$

$$lnq_e = (1/n)lnC_e + lnk_f \quad (5)$$

Langmuir isotherm adsorption model:

$$q_e = K_L q_{max} C_e/(1+K_L C_e) \quad (6)$$

$$C_e/q_e = C_e/q_{max} + 1/(K_L q_{max}) \quad (7)$$

where C_e and q_e represent the solution concentration (mg/L) and adsorption amount (mg/g) at the adsorption equilibrium state; q_{max} represents the adsorption capacity of the adsorbent (mg/g); K_f (mg/g·(L/mg)$^{1/n}$) and 1/n represent Freundlich adsorption constants, respectively, represents adsorption capacity and adsorption strength; K_L (L/mg) represents the Langmuir adsorption constant.

Figure 12 and Table 2 show the fit results of the adsorption data for the Freundlich and Langmuir isotherm models. Judging by the values of R^2, Freundlich (0.9859) is closer to 1 than Langmuir (0.9456), which means that the adsorption is more in line with Freundlich isothermal model. It belongs to multi-layer adsorption, and the adsorption sites are unevenly distributed on the surface of the adsorbent. And 1/n = 0.44 < 1, indicating that the reaction proceeds easily.

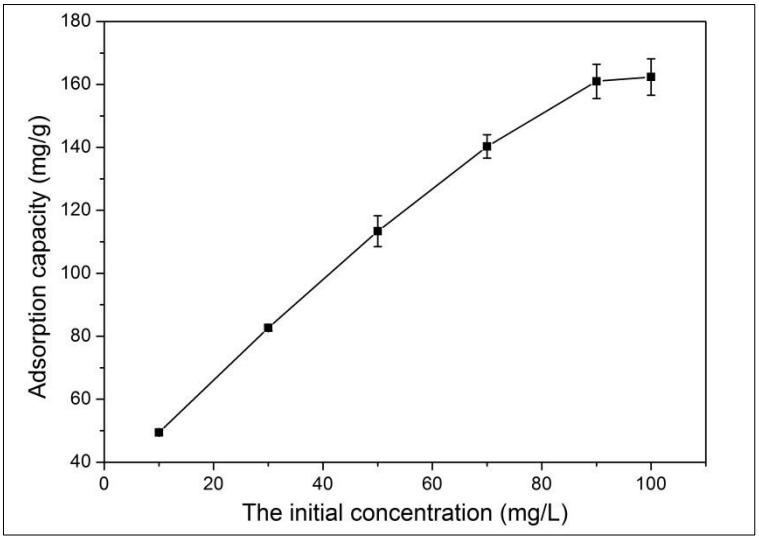

Figure 11. Effect of original Cr(VI) concentration on adsorption by PEI/MoS_2-10, solution *p*H of 2, temperature of 25°C, adsorption time of 6 h

Table 2. Freundlich and Langmuir isotherm parameters

Freundlich			Langmuir		
K_f (mg/g·(L/mg)$^{1/n}$)	1/n	R^2	q_{max} (mg/g)	K_L (L/mg)	R^2
23.29	0.44	0.9859	208.75	0.038	0.9456

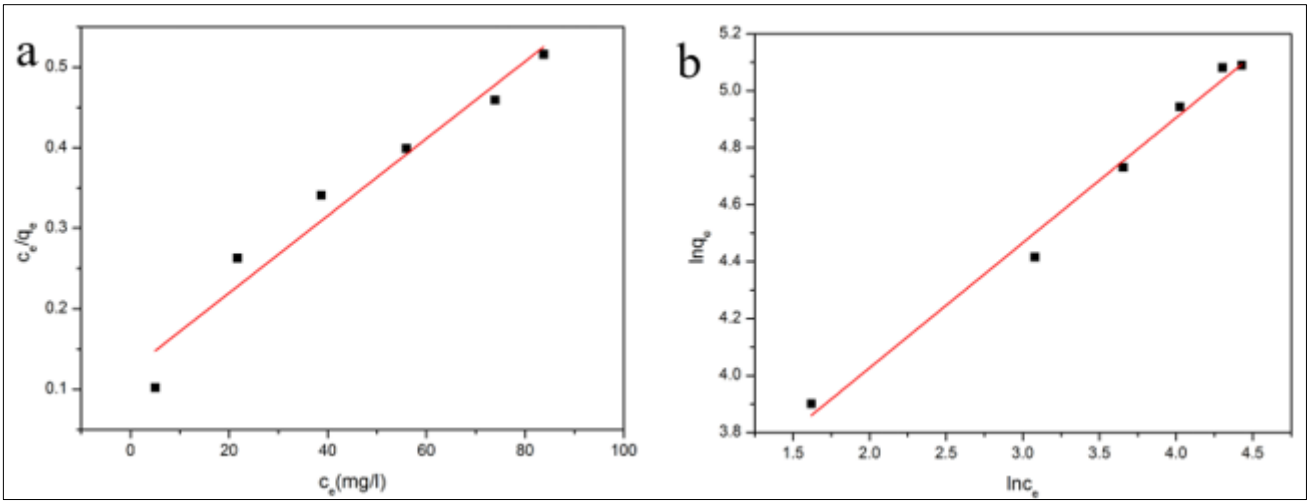

Figure 12. Adsorption isotherm fitting: a) Langmuir, b) Freundlich

3.7. Adsorption thermodynamics

Figure 13 shows the PEI/MoS_2-10 adsorption properties at 25, 30, 35, 40 and 45ºC. The higher the temperature of the solution, the greater the adsorption property of PEI/MoS2-10, which indicated that the temperature rise is promoting adsorption.

The thermodynamic properties were determined using three thermodynamic data of entropy change (ΔS^0), enthalpy change (ΔH^0) and Gibbs free energy (ΔG^0). The calculation formula is as follows:

$$ln(q_e/C_e) = -\Delta H/RT + \Delta S/R \quad (8)$$

$$\Delta G = \Delta H - T\Delta S \quad (9)$$

where R (8.3145 J/mol·K) represents the ideal gas constant, T (K) represents the absolute temperature. The values of ΔH and ΔS can be calculated from the slope and intercept of the straight line obtained by plotting ln (q_e/C_e) against 1/T (Figure 14).

Table 3 shows the calculation results that $\Delta G < 0$, increase in adsorption is spontaneous, and that the ΔG decreases as the temperature increases, showing that the temperature rise is promoting adsorption; $\Delta H > 0$ shows that the adsorption process is an endothermic reaction, and the increase in temperature is beneficial for the adsorption; $\Delta S > 0$, indicating that the disorder increased during the adsorption process.

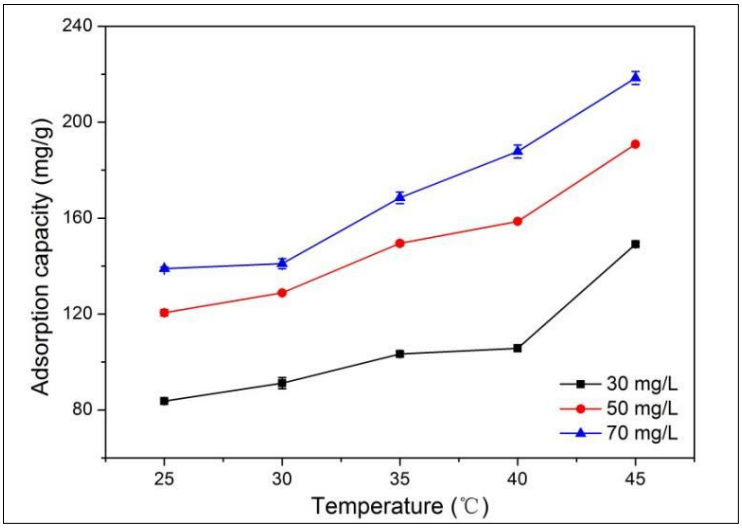

Figure 13. Effect of temperature on Cr(VI) adsorption, T = 6 h, initial Cr(VI) is 30, 50, 70 mg/L

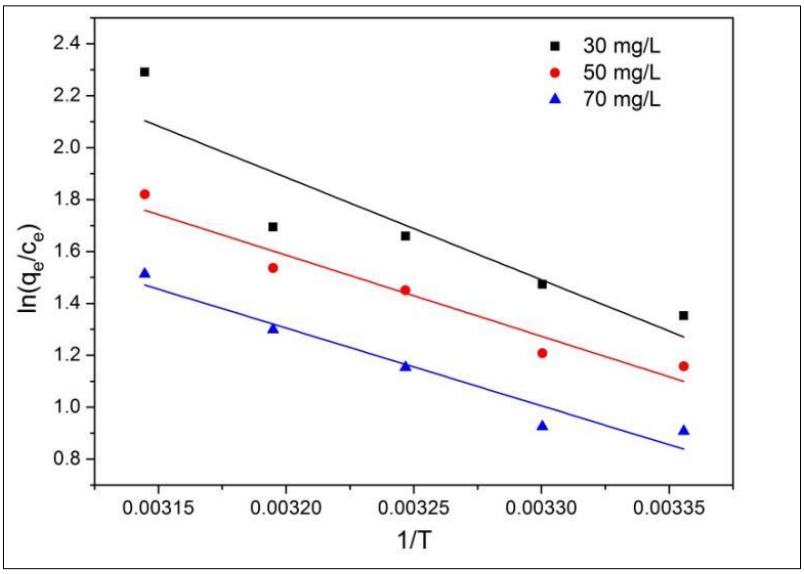

Figure 14. Van't Hoff plot

Table 3. Thermodynamics parameters

C_0 (mg/L)	Temperature (K)	ΔG (kJ/mol)	ΔH (kJ/mol)	ΔS (J/mol·k)
30	298	-3.1487	32.8197	120.70
	303	-3.7521		
	308	-4.3556		
	313	-4.9591		
	318	-5.5626		
50	298	-2.7602	25.4063	94.52
	303	-3.2327		
	308	-3.7053		
	313	-4.1779		
	318	-4.6505		
70	298	-2.0776	24.9092	90.56
	303	-2.5304		
	308	-2.9832		
	313	-3.4360		
	318	-3.8888		

3.8. Reusability test

The regeneration performance of the PEI/MoS_2-10 composite adsorbent was performed at a solution *p*H = 2 and an initial Cr(VI) concentration of 50 mg/L. After adsorption equilibrium, PEI/MoS_2-10 was repeatedly eluted three times with a 0.1 mol/L NaOH solution, washed several times with deionized water till to neutrality, and then dried for the next adsorption experiment. Repeat the adsorption-desorption four times, and the results are shown in Figure 15. After being reused four times, the adsorption capacity of PEI/MoS_2-10 still maintained more than 86%, indicating that PEI/MoS_2-10 has high reusability.

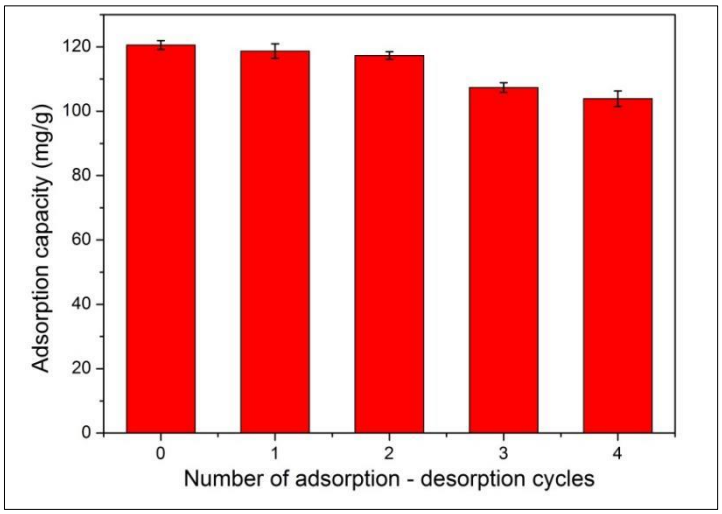

Figure 15. Cyclic tests of PEI/MoS_2-10, T = 6 h, temperature of 25°C, initial Cr(VI) is 50 mg/L

3.9. Adsorption mechanism

Figure 16 shows the XPS characterization spectra of Cr 2p after Cr(VI) adsorption by PEI/MoS_2-10. As shown in the igure, 587.63 eV and 586.57 eV correspond to the Cr 2p1/2 orbit and 578.12 eV and 577.08 eV correspond to the Cr 2p3/2 orbit. The deconvolution of the Cr2p XPS peaks is specified as the peak of 587.63 eV, 578.12 eV for Cr(VI) and 586.57 eV, 577.08 eV for Cr(III). The existence of Cr(III) confirmed that some Cr(VI) ions were reduced to Cr(III) ions after being adsorbed. This is because the nitrogen atoms in the amino and imino groups on the surface of the PEI/MoS_2-10 have lone pair electrons and have a certain reducing property, which can reduce the Cr(VI) to Cr(III). Therefore, it is speculated that the adsorption process is: (1) the positively charged amino and imino groups adsorb the negatively charged Cr(VI) onto the PEI/MoS_2-10 by electrostatic interaction; (2) Cr(VI) are reduced to Cr(III) by amino and imino groups. Its adsorption process is shown below.

$$-NH_2 + H_3O^+ + HCrO_4^- \rightarrow -NH_3^{+\cdots}HCrO_4^- + H_2O \quad (10)$$

$$= NH + H_3O^+ + HCrO_4^- \rightarrow =NH_2^{+\cdots}HCrO_4^- + H_2O \quad (11)$$

$$HCrO_4^- + 3e^- + 7\,H^+ \rightarrow Cr^{3+} + 4H_2O \quad (12)$$

$$Cr_2O_7^{2-} + 6e^- + 14\,H^+ \rightarrow 2Cr^{3+} + 7H_2O \quad (13)$$

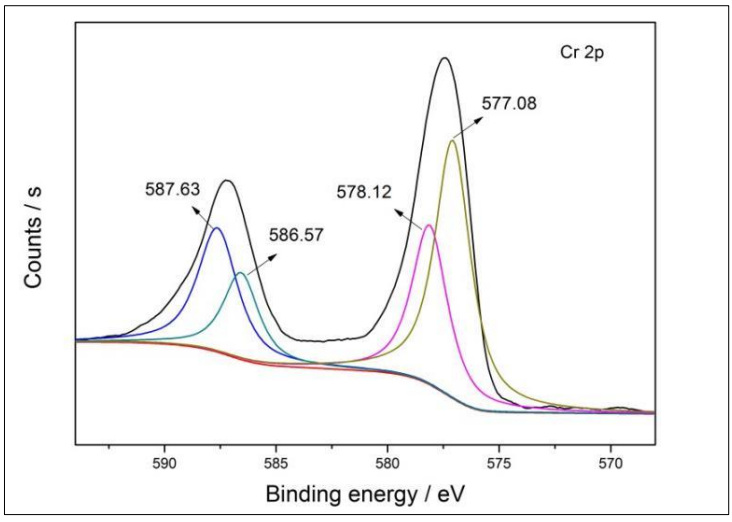

Figure 16. Binding spectrum of Cr 2p containing chromium

4. Conclusions

In this study, PEI/MoS_2 composites were successfully prepared by modifying the flower MoS_2 with polyethyleneimine (PEI). The experimental results show that PEI/MoS_2-10 has strong Cr(VI) ion enrichment ability. When the solution temperature is 25°C, the solution *p*H is 2, the concentration of PEI/MoS_2 composites adsorbent and Cr(VI) solution are 0.1 g/L and 50 mg/L, respectively, the adsorption amount of Cr(VI) ions by PEI/MoS_2-10 is 120.7 mg/g. Experiments show that PEI/MoS_2-10 has a strong selectivity to Cr(VI), and regeneration experiments show that PEI/MoS_2-10 has a high reusable, which is promising for removing and recovering Cr(VI) from the aqueous solution.

Acknowledgment: The authors would like to gratefully appreciate the financial support of this work from National Natural Science Foundation of China (No. 21676133), Natural Science Foundation of Fujian Province (No. 2021J01990), and Natural Science Foundation of Fujian Province (No. 2021J05192). The authors also express their sincere gratitude to anonymous referees for comments on this manuscript.

References

1.GUO, Y., YANG, S., Heavy metal enrichments in the Changjiang (Yangtze River) catchment and on the inner shelf of the East China Sea over the last 150 years, Sci. Total Environ., **543**, 2016, 105-115.
2.HUANG, Y. Y., ZHOU, B. H., NAN, L., LI, Y. M., HAN, R. R., QI, J. C., LU, X. H., LI, S., FENG, C. Y., LIANG, S., Spatial-temporal analysis of selected industrial aquatic heavy metal pollution in china, J. Clean. Prod., **238**, 2019, 117944.
3.HELENA, O., Chromium as an environmental pollutant: insights on induced plant toxicity, J. Bot., **2012**, 2012, 1-8.
4.HAMILTON, E. M., YOUNG, S. D., BAILEY, E. H., WATTS, M. J., Chromium speciation in foodstuffs: a review, Food Che., **250**, 2018, 105-112.
5.OWLAD, M., AROUA, M. K., DAUD, W. A. W., BAROUTIAN, S., Removal of hexavalent chromium- contaminated water and wastewater: a review, Water Air Soil Poll., **200**, 2009, 59-77.
6.DHARNAIK, A. S., GHOSH, P. K., Hexavalent chromium [Cr(VI)] removal by the electrochemical ion-exchange process, Environ. Technol., **35**(18), 2014, 2272-2279.
7.JAFARI, A. J., GOLBAZ, S., KALANTARY, R. R., Treatment of hexavalent chromium by using a combined fenton and chemical precipitation process, J. Water Reuse Desal., **3**, 2013, 373-380.
8.VENKATESWARAN, P., PALANIVELU, K., Studies on recovery of hexavalent chromium from plating wastewater by supported liquid membrane using trinbutyl phosphate as carrier, Hydrometallurgy, **78**, 2005, 107-115.
9. LI, Z. Y., HU, S., Removal of hexavalent chromium from aqueous solutions by ion-exchange resin. Adv. Mat. Res., **550-553**, 2012, 2333-2337.
10. MAMAIS, D., NOUTSOPOULOS, C., KAVALLARI, I., NYKTARI, E., KALDIS, A., PANOUSI, E., NIKITOPOULOS, G., ANTONIOU, K., NASIOKA, M., Biological groundwater treatment for chromium removal at low hexavalent chromium concentrations, Chemosphere, **152**, 2016, 238-244.
11.LIANG, H. X., SONG, B., PENG, P., JIAO, G. J., YAN, X., SHE, D., Preparation of three-dimensional honeycomb carbon materials and their adsorption of Cr(VI), Chem. Eng. J., **367**, 2019, 9-16.
12.ZHANG, S. J., SHI, Q. T., KORFIATIS, G., CHRISTODOULATOS, C., WANG, H. J., MENG, X. G., Chromate removal by electrospun PVA/PEI nanofibers: adsorption, reduction, and effects of co-existing ions, Chem. Eng. J., **387**, 2020, 124179.
13.KHANDELWAL, N., SINGH, N., TIWARI, E., DARBHA, G. K., Novel synthesis of a clay supported amorphous aluminum nanocomposite and its application in removal of hexavalent chromium from aqueous solutions, RSC Adv., **9**, 2019, 11160-11169.

14.JAHANGIRI, K., YOUSEFI, N., GHADIRI, S. K., FEKRI, R., BAGHERI, A., TALEBI, S. S., Enhancement adsorption of hexavalent chromium onto modified fly ash from aqueous solution; optimization; isotherm, kinetic and thermodynamic study, J. Disper. Sci. Technol., **2018**, 2018, 1-12.
15.ENNIYA, I., RGHIOUI, L., JOURANI, A., Adsorption of hexavalent chromium in aqueous solution on activated carbon prepared from apple peels, Sustain. Chem. Pharm., **7**, 2018, 9-16.
16.RAI, M. K., SHAHI, G., MEENA, V., MEENA, R., CHAKRABORTY, S., SINGH, R. S., RAI, B. N., Removal of hexavalent chromium Cr(VI) using activated carbon prepared from mango kernel activated with H_3PO_4, Resour. Effi. Technol., **2**, 2016, 63-70.
17.FAN, H. L., REN, H. Y., MA, X. Z., ZHOU, S. F., HUANG, J., JIAO, W. Z., QI, G. S., LIU, Y. Z., High-gravity continuous preparation of chitosan-stabilized nanoscale zerovalent iron towards Cr(VI) removal, Chem. Eng. J., **390**, 2020, 124639.
18.QUAN, G., ZHANG, J., GUO, J., LAN, Y., Removal of Cr(VI) from Aqueous Solution by Nanoscale Zero-Valent Iron Grafted on Acid-Activated Attapulgite, Water Air Soil Poll., **225**, 2014, 1979.
19.GAFFER, A., KAHLAWY, A. A. A., AMAN, D., Magnetic zeolite-natural polymer composite for adsorption of chromium (VI), Egypt. J. Pet., **2**, 2017, 995-999.
20. KRISHNANI, K. K., SRINIVES, S., MOHAPATRA, B. C., BODDU, V. M., HAO, J., MENG, X., MUCHANDANI, A., Hexavalent chromium removal mechanism using conducting polymers, J, Hazard, Mater., **252-253**, 2013, 99-106.
21.CHHOWALLA, M., SHIN, H. S., EDA, G., LI, L. J., LOH, K. P., ZHANG, H., The chemistry of two-dimensional layered transition metal dichalcogenide nanosheets, Nat. Chem., **5**, 2013, 263-275.
22.MURATORE, C., VOEVODIN, A. A., Molybdenum disulfide as a lubricant and catalyst in adaptive nanocomposite coatings, Surf. Coat. Tech., **201**, 2006, 4125-4130.
23.FARSADI, M., BAGHERI, S., ISMAIL, N. A., Nanocomposite of functionalized graphene and molybdenum disulfide as friction modifier additive for lubricant, J. Mol. liq., **244**, 2017, 304-308.
24.FENG, C., MA, J., LI, H., ZENG, R., GUO, Z., LIU, H., Synthesis of molybdenum disulfide (MoS_2) for lithium ion battery applications, Mater. Res. Bull., **44**(9), 2009, 1811-1815.
25.GHANEI-MOTLAGH, M., TAHER, M. A., A novel electrochemical sensor based on silver/ halloysite nanotube/molybdenum disulfide nanocomposite for efficient nitrite sensing, Biosens. Bioelectron., **109**, 2018, 279-285.
26.JIA, F., LIU, C., YANG, B., ZHANG, X., YI, H., NI, J., SONG, S., Thermal modification of molybdenum disulfide surface for tremendous improvement of Hg^{2+} adsorption from aqueous solution, ACS Sustain. Chem. Eng., **6**, 2018, 9065-9073.
27. CHAO, Y., ZHU, W., WU, X., HOU, F., XUN, S., WU, P., JI, H. Y., XU, H., LI, H. M., Application of graphene-like layered molybdenum disulfide and its excellent adsorption behavior for doxycycline antibiotic, Chem. Eng. J., **243**, 2014, 60-67.
28.HUANG, Q., ZHAO, J., LIU, M. Y., Synthesis of polyacrylamide immobilized molybdenum disulfide (MoS_2@PDA@PAM) composites via mussel-inspired chemistry and surface-initiated atom transfer radical polymerization for removal of copper (II) ions, J. Taiwan Inst. Chem. E., **86**, 2018, 174-184.
29.CHEN, X., BERNER, N. C., BACKES, C., DUESBERG, G. S., MCDONALD, A. R., Functionalization of two-dimensional MoS_2: on the reaction between MoS_2 and organic thiols, Angew. Chem. Int. Ed., **55**(19), 2016, 5803-5808.
30. YANG, X., MENG, N. N., ZHU, Y. C., ZHOU, Y. F., NIE, W. Y., CHEN, P. P., Greatly improved mechanical and thermal properties of chitosan by carboxyl-functionalized MoS_2 nanosheets, J. Mater. Sci., **51**, 2016, 1344-1353.
31.AGHAGOLI, M. J., SHEMIRANI, F., Hybrid nanosheets composed of molybdenum disulfide and reduced graphene oxide for enhanced solid phase extraction of Pb(II) and Ni(II), Microchim. Acta, **184**, 2017, 237-244.

32.LU, Y., FANG, Y. Y., XIAO, X. D., QI, S., HUAN, C. M., ZHAN, Y. J., CHENG, H. L., XU, G., Petal-like molybdenum disulfide-loaded nanofibers membrane with superhydrophilic property for dye adsorption, Colloids Surf., A, **553**, 2018, 210-217.
33.BAO, S. T., YANG, W. W., WANG, Y. J., YU, Y. S., SUN, Y. Y., LI, K. F., PEI grafted amino-functionalized graphene oxide nanosheets for ultrafastand high selectivity removal of Cr(VI) from aqueous solutions by adsorptioncombined with reduction: Behaviors and mechanisms, Chem. Eng. J., **399**, 2020, 125762.
34.CHEN, B., ZHAO, X., LIU, Y., XU, B., PAN, X., Highly stable and covalently functionalized magnetic nanoparticles by polyethyleneimine for Cr(VI) adsorption in aqueous solution, RSC Adv., **5**, 2014, 1398-1405.
35.CHEN, Y., PAN, R., RNHAIYAN, L. I., ZHANG, R., RNLU, L. V., RNJUN. W. U., Selective removal of Cu(II) ions by using cation-exchange resin-supported polyethyleneimine (PEI) nanoclusters, Environ. Sci. Technol., **44**, 2010, 3508-3513.
36.JIANG, H., SUN, M., XU, J., LU, A., SHI, Y., Magnetic Fe_3O_4 nanoparticles modified withpolyethyleneimine for the removal of Pb(II), CLEAN-Soil Air Water, **44**, 2016, 1146-1153.
37.GUO, D. X., SONG, X. M., ZHANG, L. L., CHEN, W. W., CHU, D. W., TAN, L. C., Recovery of uranium(VI) from aqueous solutions by the polyethyleneimine-functionalized reduced graphene oxide/molybdenum disulfide composition aerogels, J. Taiwan. Inst. Chem. E., **106**, 2020, 198-205.
38.GENG, J. J., YIN, Y. W., LIANG, Q. W., ZHU, Z. J., LUO, H. J., Polyethyleneimine cross-linked graphene oxide for removing hazardous hexavalent chromium: Adsorption performance and mechanism, Chem. Eng. J., **361**, 2019, 1497-1510.
39.SAHA, B., ORVIG, C., Biosorbents for hexavalent chromium elimination from industrial and municipal effluents, Coordin. Chem. Rev., **254**, 2010, 2959-2972.

Manuscript received: 6.12.2021